Characterizing the Respiratory Artefact in Functional MRI

M. P. Griffin[1], B. Pike[1]

[1]Montreal Neurological Institute, McGill University, Montreal, Quebec, Canada

Introduction Respiratory artefacts are a major cause of noise in functional MRI studies [1]. These artifacts are generally attributed to bulk susceptibility changes or to head motion [2], and are best described in images of the amplitude of respiratory fluctuations in the phase of the MR signal [3]. Such images possess an even smoothly varying structure, and are in excellent qualitative agreement with numerical simulations described by Raj [4] where for a single point source the amplitude of the respiratory fluctuations falls off as $1/r^3$. A number of algorithms have been proposed for characterizing and removing this artefact which exploit this smooth structure to full advantage. One successful example is the use of navigator echo techniques [5], which generally assume that there is no significant variation in the respiratory artefact across each slice. Another important application is in multi-slice acquisitions, where there is not sufficient temporal resolution to sample each slice within Nyquist limits. Frank [6] has proposed a technique for solving this problem by assuming that the respiratory fluctuations have an equal amplitude in each voxel across the acquisition. Our interest in characterizing the respiratory artefact comes from developing software capable of simulating the signal and artifacts present in realistic fMRI data (for this purpose a full-brain characterization of the artefact was essential). The work described in this current abstract aims to provide a thorough and quantative foundation for the choice of functional representations used to describe the respiratory artefact.

Methods MRI scans were performed on six healthy volunteers with a Siemens 1.5T Sonata MR Scanner (Siemens Medical Systems, Erlangen, Germany). Resting state data was acquired using a standard EPI sequence and the magnitude and phase images were reconstructed. Each run consisted of 750 measurements and 10 slices (with a slice gap of 12mm in order to achieve full-brain coverage). 6.25mm isotropic voxels were acquired with TR/TE/flip angle = 464ms/12ms/50º. The low TE was chosen to reduce contamination from dominant field susceptibilities at the base of the brain, and hence to allow the respiratory effect to be quantified in these regions. Slices were angled AC-PC to further reduce susceptibility artifacts from the sinuses (though this may have repercussions for the fitting of 2D polynomials of order 1). A fourier transform was performed on the timecourse of the phase from each voxel, and summed across a small frequency range containing the dominant respiratory frequency (in a manner previously described by Windischberger [6]). This measure, termed the Area Under the Curve [6], is a relative measure describing the size of the respiratory fluctuation, and was normalized against the mean AUC over the brain. Three-dimensional polynomials of order 0 to 5 were then fit to the AUC image of each patient. As a separate experiment, two-dimensional polynomials were fit to each individual slice. Goodness of fit measures (χ^2) were then determined for each functional representation.

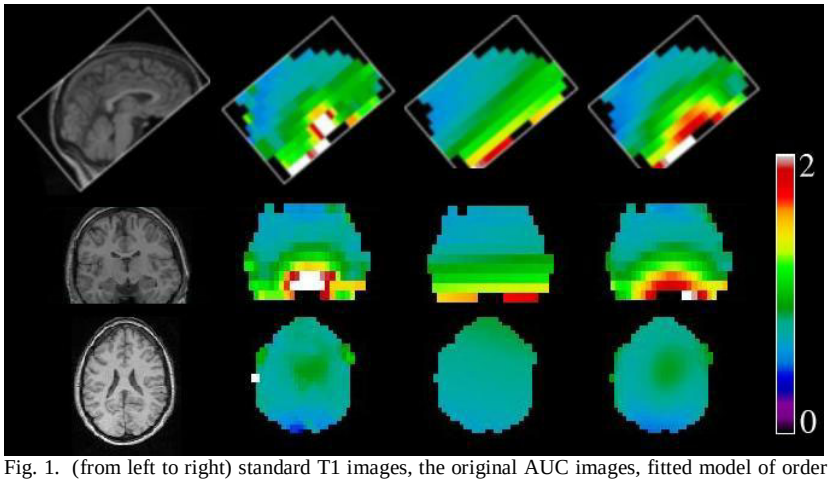

Fig. 1. (from left to right) standard T1 images, the original AUC images, fitted model of order 1, and fitted model of order 4. Note that images are acquired AC-PC

Results Figure 1 shows the AUC images produced in this study from a typical subject, along with the results of fitting 2D polynomials of orders 1 and 4 to each slice of the AUC. Figure 2 shows the χ^2 measures obtained from fitting 2D polynomials on a slice by slice basis, and 3D polynomials to each volume (results are shown as the median result over all subjects).

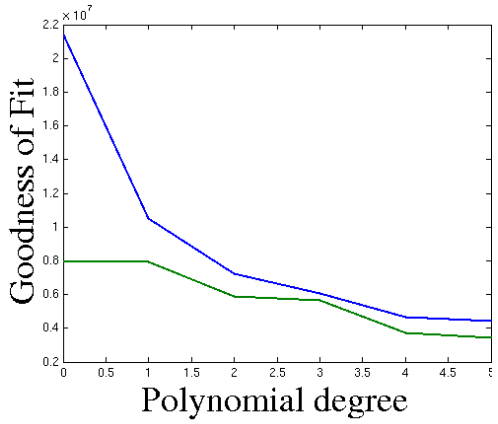

Fig. 2. The goodness of fit resulting from fitting polynomials of various orders to the AUC images (3D polynomials in blue, 2D in green). Results are shown as the median result over all subjects.

Discussion A number of techniques have been proposed in the literature for characterizing and removing respiratory artefacts. These algorithms often rely on assumed functional representations of these artefacts. The goal of the work presented herein is to provide a numerical justification for the assumptions made. One can see in Figure 1 that the major component of the respiratory artefact is at the base of the brain and falls off roughly in the axial direction. This is also evidenced in Figure 2 where the 2D polynomials provide a significantly better goodness of fit than 3D polynomials of the same order. It is interesting to note that while the normalized χ^2 reaches a plateau around 0.4×10^7, that the χ^2 obtained when fitting a 3D polynomial of order 0 is approximately five times larger than that (with distinct repercussions for multi-slice acqusitions). It is also interesting to not that the χ^2 values obtained from 2D polynomials are approximately twice as large for 0 degree polynomials compared to higher degrees. In addition it can be seen that while cubic polynomials are a good match for the data as predicted in the numerical simulations performed by Raj [4], that there is some added complexity in the geometry of the human respiratory system.

Conclusions The extent to which polynomials of various orders captured the structure of the respiratory artefact was assessed through constructing AUC images. The major variation in the respiratory artefact is along the axial direction (as has previously been well described) and hence for low order polynomials 2D polynomials fit to each slice greatly out-perform 3D polynomials fit to the volume. For 2D polynomials there is approximately a 50% improvement in using high-order expansions, the saving is much greater when using 3D polynomials. Such savings suggest that a major improvement in the removal of respiratory artefacts will come from the development of techniques which make use of these higher order functional forms.

References

[1] Weisskoff *et al. Proc. ISMRM* 1993:7. [2] Brosch *et al. IEEE Trans. Biomed. Eng.*, 49:700-707, 2002. [3] Noll *et al. Proc IEEE Internat. Conf. Image Proc.*, 40-44, 1994. [4] Raj *et al. Phys. Med. Biol.*, 45:3809-3820, 2000. Kim *et al. MRM* 13:25-37, 1990. [5] Frank *et al. MRM* 45:635-644, 2001. [6] Windischberger *et al. MRI*, 20:575-582, 2002.